Introgression across semipermeable species boundaries within the *Sebastes inermis* complex

Diego Deville [1], **Kentaro Kawai** [1], **Hiroki Fujita** [2], **Tetsuya Umino** [Corresp. 1]

[1] Graduate School of Integrated Sciences for Life, Hiroshima University, Higashihiroshima, Hiroshima, Japón

[2] Seto Marine Biological Laboratory, Field Science Education and Research Center, Kyoto University, Shirahama, Wakayama, Japan

Corresponding Author: Tetsuya Umino
Email address: umino@hiroshima-u.ac.jp

Introgression can have important implications for speciation either by promoting the emergence of novel adaptations or reinforcing the boundaries between parent species. The semipermeable nature of species boundaries, as supported by the occurrence of introgression, indicates that it typically does not occur in genomic regions under strong divergent selection, which are crucial to speciation. In this sense, we assessed the dynamics of introgression and genetic divergence within the*Sebastes inermis* complex (*Sebastes cheni*, viz.*Sebastes inermis*, *Sebastes ventricosus*, and their putative morphological hybrids in sympatry) using a dataset of 10 microsatellite loci, mitochondrial DNA (D-loop), and the intron-free rhodopsin gene (RH1). The analyses revealed the presence of three distinct genetic clusters, large genetic distances in the D-loop region, and the presence of RH1 mutations, which align with the description of each species. Two of the microsatellite loci showed evidence of divergent selection indicating that they are linked to genomic regions crucial for speciation. Furthermore, nonsynonymous RH1 mutations detected in *S. cheni* and the "Kumano" morphotype, a putative morphological hybrid, suggest specific adaptations related to visual perception in dim light environments. The occurrence of introgression was confirmed through individual admixture coefficients and significant migration rates between species. The admixture coefficients were effective in distinguishing genetically pure individuals and first-generation hybrids, but they were unable to identify backcrosses. The presence of nonsynonymous RH1 mutations and the admixed genetic ancestry of the "Kumano" morphotype, along with the independent divergence of each species highlight the significant role of introgression in relation to speciation within the*Sebastes inermis* complex. Our findings emphasize the need for further studies to assess the relative fitness of hybrids and parentals, particularly in the context of stock enhancement programmes for the three species since they can potentially increase the chances of introgression and its consequences within the species complex.

Introgression across semipermeable species boundaries within the *Sebastes inermis* complex

Diego A. Deville [1], Kentaro Kawai [1], Hiroki Fujita [2], Tetsuya Umino [1]

[1] Graduate School of Integrated Sciences for Life, Hiroshima University, Higashihiroshima, Hiroshima 739-8528, Japan.

[2] Seto Marine Biological Laboratory, Field Science Education and Research Center, Kyoto University, 459 Shirahama, Wakayama, 649-2211, Japan.

Corresponding Author:

Tetsuya Umino [1]

Graduate School of Integrated Sciences for Life, Hiroshima University, Higashihiroshima, Hiroshima 739-8528, Japan.

Email address: umino@hiroshima-u.ac.jp

Abstract

Introgression can have important implications for speciation either by promoting the emergence of novel adaptations or reinforcing the boundaries between parent species. The semipermeable nature of species boundaries, as supported by the occurrence of introgression, indicates that it typically does not occur in genomic regions under strong divergent selection, which are crucial to speciation. In this sense, we assessed the dynamics of introgression and genetic divergence within the *Sebastes inermis* complex (*Sebastes cheni*, viz. *Sebastes inermis*, *Sebastes ventricosus*, and their putative morphological hybrids in sympatry) using a dataset of 10 microsatellite loci, mitochondrial DNA (D-loop), and the intron-free rhodopsin gene (RH1). The analyses revealed the presence of three distinct genetic clusters, large genetic distances in the D-loop region, and the presence of RH1 mutations, which align with the description of each species. Two of the microsatellite loci showed evidence of divergent selection indicating that they are linked to genomic regions crucial for speciation. Furthermore, nonsynonymous RH1 mutations detected in *S. cheni* and the "Kumano" morphotype, a putative morphological hybrid, suggest specific adaptations related to visual perception in dim light environments. The occurrence of introgression was confirmed through individual admixture coefficients and significant migration rates between species. The admixture coefficients were effective in distinguishing genetically pure individuals and first-generation hybrids, but they were unable to identify backcrosses. The presence of nonsynonymous RH1 mutations and the admixed genetic ancestry of the "Kumano" morphotype, along with the independent divergence of each species highlight the significant role of introgression in relation to speciation within the *Sebastes inermis* complex. Our findings emphasize the need for further studies to assess the relative

fitness of hybrids and parentals, particularly in the context of stock enhancement programmes for the three species since they can potentially increase the chances of introgression and its consequences within the species complex.

Introduction

Natural hybridization involves the exchange of genetic material between different populations or taxa. Introgression refers to the transfer of alleles from one genetically distinct taxon into the gene pool of another taxon through subsequent backcrossing (Anderson, 1949). Introgression challenges the traditional biological species concept, which defines species as reproductively isolated from one another (Mayr, 1963). However, a "genic view" of species proposed by Wu - - (2001) offers an alternative perspective. According to this view, gene flow can occur among species if the parent species maintain their divergence upon contact (*i.e.*, speciation-with-gene-flow). In this framework, reproductive isolation is only applied to genes involved in speciation rather than being considered a whole-genome phenomenon.

In the process of speciation-with-gene-flow, species divergence primarily occurs in specific genomic containing genes that are under strong divergent selection and play a crucial role in local adaptation and speciation (Via, 2001). Conversely, other genomic regions that are weakly selected or neutral and not essential for maintaining species boundaries can be freely exchanged during gene flow between species (Shaw & Mullen, 2011; Feder, Egan & Nosil, 2012). The differential patterns of introgression observed in these genomic regions highlight the semipermeable nature of species boundaries (Harrison & Larson, 2014). By studying these patterns, we can gain insights into the dynamics of speciation and the factors shaping species boundaries.

Possible outcomes of introgression into speciation primarily depend on the fitness of hybrids related to parent species in specific environments, and their reproductive success (Via, 2001; Baskett & Gomulkiewicz, 2011). A higher fitness of hybrids may have significant evolutionary potential to generate novel lineages and/or adaptations (Arnold, 1992; Arnold & Fogarty, 2009; Abbott et al., 2013). Conversely, if hybrids have lower fitness than the parent species, introgression can contribute to increasing the reproductive isolation of the hybridizing lineages (*i.e.*, reinforcement) (Dobzhansky, 1940; Servedio & Noor, 2003). In this sense, the occurrence of introgression in a single clade offers the possibility of directly assessing the hybrids fitness and the significant contribution of both possible outcomes of introgression on diversification.

The species complex *Sebastes inermis* encompasses three species: viz. *Sebastes inermis* Cuvier, 1829 (red-coloured), *Sebastes cheni* Barsukov, 1988 (brown to golden-brown rockfish, known as "white" in Japan), and *Sebastes ventricosus* Temminck & Schlegel, 1843 (greenish- to black-coloured), which present extensive sympatry along coastal waters of Japan (Kai & Nakabo, 2008). Apart from their colouration patterns, the morphological identification of these species relies on meristic, and morphometric proportions (Kai & Nakabo, 2008), although additional morphological differences in otolith descriptors and body shape can ease their identification (Deville et al., 2023). These morphological divergences also suggest asymmetric depth distributions for these species, which can reduce their interspecific competition and allow their coexistence in sympatry (Deville et al., 2023). Genetic identification of these rockfishes can be accomplished by examining differences in allele patterns of Amplified Fragment Length Polymorphisms (AFLP) (Kai, Nakayama & Nakabo, 2002; Kai & Nakabo, 2008), and two microsatellite loci (Deville et al., 2023). Dissimilar allele patterns in these molecular markers suggest reproductive isolation between these species (Kai, Nakayama & Nakabo, 2002), which

93 aligns with differences in acoustic and visual communication systems that can be important for
94 the recognition of conspecifics during reproductive seasons (Deville et al., 2023). Due to the
95 economic significance of these species for local communities, thousands of juveniles from all the
96 three species are annually released into coastal waters of Japan to enhance local stocks
97 (Nakagawa, 2008). However, this practice might increase chances of introgression among these
98 species. Given that introgression can alter estimates of genetic population structure within
99 species (Berntson & Moran, 2009; Artamonova et al., 2013; Saha et al., 2017), its detection is
100 crucial to implement fishery management policies aimed at preserving the genetic diversity of
101 these species (Buonaccorsi et al., 2005; Berntson & Moran, 2009).
102 Introgression within *Sebastes* has been inferred through various methods. Morphological
103 analyses have been used to identify hybrids based on intermediate morphotypes of the parent
104 species (Valentin, Sévigny & Chanut, 2002; Muto et al., 2013). In other cases, migration rates
105 between species have been estimated using isolation with migration models under a coalescent
106 approach (Saha et al., 2017; Schwenke, Park & Hauser, 2018). In addition, introgression events
107 have been detected through population genetic surveys using highly polymorphic markers such
108 as microsatellite loci, which were analysed through Bayesian clustering methods (Roques,
109 Sévigny & Bernatchez, 2001; Buonaccorsi et al., 2005; Burford, 2009; Saha et al., 2017),
110 because these methods can determine the number of different genetic clusters and estimate the
111 contribution of each genetic cluster to an individual's ancestry (Pritchard, Stephens & Donnelly,
112 2000; Corander et al., 2008). Moreover, analyses of microsatellite loci have served as a baseline
113 for further characterization of genome-wide patterns of divergence between closely related
114 species (Buonaccorsi et al., 2011; Behrens et al., 2021) even though the high mutation rate of
115 these markers can possibly lead to the convergence of alleles between species (Estoup, Jarne &

Cornuet, 2002; Morales et al., 2021). The detection of high "outlier" genetic divergences between species in contrast to low intraspecific divergences can indicate that these loci are under adaptive (divergent) selection (*i.e.*, FST "outlier" approach) (Beaumont & Balding, 2004). When a locus is under divergent selection, alleles of any locus near linked regions will also be under divergent selection; thus, that selection will prevent gene flow of all nearby genomic regions, leading to a reduction in the migration rate (*i.e.*, gene flow) of that region (Feder, Egan & Nosil, 2012).

In the *S. inermis* complex, putative morphological hybrids displaying intermediate colouration and meristic counts, but with otolith weight ~ age relationships resembling *S. cheni*, have been categorized into any of the three species based on allele patterns of two microsatellite loci (Deville et al., 2023). Additionally, an endemic intermediate morphotype of *S. cheni* and *S. inermis* (colloquially called "big red") has been reported by local fishermen in Kumano Nada (Wakayama Prefecture), but without any genetic information. The presence of these putative morphological hybrids in sympatry, along with females' behaviour leading to assortative mating for larger males during reproductive seasons (Shinomiya & Ezaki, 1991), urge the need to confirm whether hybridization is occurring among these species.

To investigate the dynamics of introgression and genetic divergence within the *Sebastes inermis* complex, we employed genetic information from the mitochondrial control region (D-loop), the introgression-free rhodopsin gene (RH1), and 10 microsatellite loci. Our study aimed to address the following objectives:

1. Assess the genetic divergences between species in sympatry, with a particular focus on identifying nonsynonymous mutations in the intro-free rhodopsin gene (RH1). Such mutations can indicate differences in depth distribution and adaptation to environments with

varying levels of downwelling light (Bowmaker, 2008; Sivasundar & Palumbi, 2010; Shum et al., 2014).

2. Detect introgression events through clustering analyses and isolation with migration models based on a coalescent approach. These methods allow us to evaluate the extent and direction of gene flow between species.
3. Investigate whether any of the microsatellite loci show signs of divergent selection, which can provide insights into recent and local adaptation within the complex.
4. Evaluate the level of genetic divergence of the putative morphological hybrids.

Our expectations were that each species would maintain its genetic divergence even in the presence of introgression, as gene flow is typically restricted in genomic regions under divergent selection that are responsible for driving speciation. We also anticipated that the intermediate morphotypes would exhibit genetic signatures consistent with admixture of the parent species. The occurrence of introgression in sympatry would provide further evidence supporting the potential role of introgression in the diversification of *Sebastes* rockfishes.

Materials & Methods

Sampling

We examined a total of 360 rockfishes collected through bank and rock fishing activities along the coast of Japan (**Table 1**, **Fig. 1**). Species identification was carried out following the criteria established by Kai & Nakabo (2008), starting from colour alive and fresh, meristic counts, and body proportions. In addition, the otolith weight ~ age relationship was used to ensure correct identification of specimens older than 4 years old, as suggested by Deville et al. (2023).

Individuals were categorized into six different morphological groups considering whether they present all the diagnostic traits of any species without overlap or only some of them (**Table 1**, **Fig. 2**). The categories were as follows: (1) white *S. cheni*, (2) red *S. inermis*, (3) black *S.*

ventricosus, (4) intermediate black-white (BW) *S. cheni – S. ventricosus*, with some individuals having colouration from one species while their meristic counts and body proportions resemble the other species, (5) intermediate red-white (RW) *S. cheni – S. inermis*, with intermediate colouration and meristic counts, but otolith weight ~ age relationship of *S. cheni*, and (6) "Kumano" or "big red" morphotype collected in sandy and rocky shorelines in East Wakayama Prefecture. It is considered a hypothetical intermediate form between *S. inermis* and *S. cheni* that displays intermediate colouration and meristic counts, but an otolith weight ~ age relationship similar to *S. cheni*.

DNA isolation, sequencing, and genotyping

Total DNA of specimens was isolated from a small piece of fin tissue using the TNES-Urea buffer (Asahida et al., 1996) followed by the standard phenol-chloroform isolation. A set of 10 microsatellite loci isolated from *Sebastes schlegelii* Hilgendorf, 1880 (SSC12, SSC23, KSs2A, KSs6A, KSs7, and CGN1) (Yoshida, Nakagawa & Wada, 2005; An et al., 2009; Gao et al., 2018), *S. inermis* (Sebi1, Sebi2, and Sebi3) (Blanco Gonzalez et al., 2009), and *Sebastes rastregiller* (Jordan & Gilbert, 1880) (SRA7-7) (Westerman et al., 2005), were cross-amplified in all samples through two multiplex PCRs. The four universal primers proposed by Blacket et al., (2012) were labelled with 6-FAM (Tail A), VIC (B), NED (C), and PET (D), while the forward primers of all loci were modified at their 5' ends with the same universal primers (**Table S1**). Multiplex PCR standardization for these loci was performed as described in Deville et al., (2021). Each multiplex PCR was carried out in a volume of 5 µL containing 2.5 µL of 2X KOD Fx Neo buffer, 1 µL of dNTP 2µM, 0.1 µL of 1U KOD polymerase (Toyobo Co., Ltd., Osaka, Japan), 1 µL of DNA, and 0.1 µL of a primer mix (5mM labelled universal primers and modified forward primers, and 10 mM reverse primers). Multiplex PCRs were performed in a

Mastercycler Gradient 96-well system (Eppendorf, Hamburg, Germany) with initial denaturation at 94°C for 4 min followed by a touchdown (10 cycles at 94 °C/1 min, annealing from 63 °C to 54 °C/ 1 min and 72 °C/ 1 min), 20 cycles with the same conditions but annealing at 55° C and a final step of 72°C during 10 min. Then 1 µL of PCR products was mixed with 18.8 µL of Hi-DiTM Formamide (Applied Biosystem) and 0.2 µL of GeneScanTM-600 LIZ ® size standard (Applied Biosystem). This mixture was denatured at 95 °C for 3 min and run on an ABI 3130×1 Genetic Analyzer (Applied Biosystems). Genotyping was performed using GeneMarker v.2.6 ® (Soft Genetics).

D-loop and the RH1 gen were amplified in 130 specimens, including: (1) 25 individuals of each species identified through morphological and genetic analyses (clustering analysis, see below); (2) eight individuals morphologically assigned to a species but genetically classified as putative hybrids; (3) 22 individuals with BW morphotype, (4) 19 specimens showing RW morphotype, and (5) six "Kumano" specimens from Wakayama. D-loop was amplified using the forward (MebTD1F, 5'→3': ACCTGAATCGGAGGAATGCC) and reverse (MebTD1R, 5'→3': GGGTTTACAGGAGCGTTAGC) primers designed in this study. RH1 was amplified using the Rh193 (5'→3': CNTATGAATAYCCTCAGTACTACC) and Rh1039r (5'→3': TGCTTGTTCATGCAGATGTAGA) primers (Chen, Bonillo & Lecointre, 2003). Both genetic regions were amplified in a total volume of 8 µL containing 4 µL of 2X KOD buffer, 1.2 µL of dNTP 2µM, 0.1 µL of each primer, 0.1 µL of 1U KOD Taq polymerase, and 1 µL of DNA. PCR conditions for both regions were: initial denaturation at 94 °C for 4 min and then 35 cycles of 94 °C for 20 seg, 55 °C for 30 seg and 68 °C for 45 seg, and a final extension at 68 °C for 5 min. Each PCR product was cleaned up with ExoSAP-IT (Affymetrix/USB Corporation, Cleveland, OH) and then sequenced using BigDye v3.1 Terminator Sequencing Kit (Applied Biosystems)

on a Genetic Analyzer ABI 3130x1 (Applied Biosystems). D-loop amplicons were sequenced in one direction, whereas RH1 amplicons were sequenced in both directions whenever an ambiguous nucleotide was found in the chromatograms. Chromatograms were visualized and manually edited using Chromas lite v2.6.6 (Technelysium Pty. Ltd.) and the sequences were aligned using Clustal X2 (Larkin et al., 2007). RH1 sequences were phased into two sequences per individual using the program PHASE implemented in DNAsp v6 (Rozas et al., 2017) with a Markov chain Monte Carlo of 100,000 iterations, burn-in of 10,000 steps, and 10 step thinning intervals.

Descriptive statistics and genetic divergences

We estimated the number of alleles (Na), observed heterozygosity (Ho), and expected heterozygosity (He) for each species. Exact tests for Hardy-Weinberg equilibrium (HWE) and linkage disequilibrium were performed for each locus and pair of loci, respectively. These tests were performed per species and only in eight populations (two populations of *S. cheni* and three populations of *S. inermis* and *S. ventricosus*) containing more than 25 individuals. Pairwise genetic divergences between species were estimated based on the number of different alleles (Weir & Cockerham, 1984) only using individuals from Hiroshima whose identity was confirmed through morphological and genetic analyses (see clustering analysis). All these analyses were performed using Arlequin v3.5 (Excoffier & Lischer, 2010).

D-loop and phased RH1 haplotypes were collapsed into haplotypes, and the number of haplotypes, haplotype diversity, and nucleotide diversity were estimated using DNAsp v6. Genetic distances between species from frequencies of D-loop haplotypes were estimated using the K2P model (Kimura, 1980) in Arlequin v3.5. Networks of D-loop and RH1 haplotypes were constructed using the TCS method (Clement, Posada & Crandall, 2000) implemented in PopArt

v1.7 (Leigh & Bryant, 2015). To determine the position of mutations occurring in the RH1 gene and their possible relationship with changes in the protein function, we selected the individual with the longest sequences in each species and pooled them together with the publicly available RH1 sequences of 36 *Sebastes* rockfishes (EF212407–EF212438, KM013899, KM013904, KM013924, KM013927), using as reference the complete amino acid sequence of the bovine RH1 (GenBank accession NM_001014890).

Detection of outlier loci

Outlier loci with very low or high divergence among species were detected using BayeScan v2.1. (Foll & Gaggiotti, 2008). The analysis was performed only with the allele frequencies of individuals assigned to a species based on their morphology. The parameters for the analysis were as follows: 100,000 burn-in steps, a thinning interval of 100, a sample size of 10,000, 50 pilot runs, a pilot length of 10,000, and a value of 10 for prior odds. The analysis assesses selection by decomposing FST coefficients into a population-specific component (beta) shared by all loci and a locus-specific component (alpha) shared by all populations using logistic regression. Loci under selection are inferred when FST coefficients are largely explained by the locus-specific component (*i.e.*, alpha is significantly different from 0). Positive alpha values indicate divergent selection, whereas negative values suggest balancing or purifying selection. The significance of each alpha value per locus was evaluated using corrected *P* values calculated using the False Discovery Rate method (FDR) (Benjamini & Hochberg, 1995).

Genetic clusters and individual admixture analysis from microsatellite loci

Genetic clustering was assessed using STRUCTURE v2.3.4 (Pritchard, Stephens & Donnelly, 2000). The analysis estimated the number of different genetic clusters and individual admixture proportions (Q-score = genome ancestry coefficient) to identify possible hybrids. Two analyses

were performed: the first using all microsatellite loci and the second excluding loci under putative divergent selection. The analyses were run with a Markov chain Monte Carlo of 1,000,000 steps, 10% burn-in, independent allele frequency model, K (number of possible clusters) values from 1 to 7, and 10 replicates for each K value. The most likely number of genetic clusters was inferred using the Evanno method (Evanno, Regnaut & Goudet, 2005), as implemented in STRUCTURE HARVESTER (Earl & vonHoldt, 2012). Putative genetic hybrids were identified through individual admixture proportions (hereafter Q-scores) considering values lower than 0.9 (Sanz et al., 2009).

Thirty individuals with unequivocal morphological definition and Q-scores higher than 0.99 were used as reference populations for simulating pure, first-generation (F1) hybrids, and backcross individuals using HYBRIDLAB v1.0 (Nielsen et al., 2006). A total of 810 pure parental genotypes were simulated by simple mechanical mixing of the alleles from each pure reference population. For F1 hybrids, we simulated 30 individuals for each parent cross: *S. cheni – S. inermis*, *S. cheni – S. ventricosus*, and *S. inermis – S. ventricosus*. For the backcrosses, 30 individuals were simulated for each pure parental and F1 cross, resulting in six groups of backcrosses. Each group was labelled with three letters following the colour pattern of each parent species (*i.e.*, black: B, red: R, and white: W) to ease their distinction. The first and second letters indicate the origin of the F1 hybrid parental, and the third letter indicates the parental of pure origin. The six groups of backcrosses were BRB, BRR, BWB, BWW, RWR, and RWW. The number of simulated individuals in the pure, F1 hybrid, and backcrossing groups was set to ensure 10% of hybrids in our simulated dataset as a requirement to effectively infer hybrids using clustering analyses (Vähä & Primmer, 2006). We pooled the simulated individuals in a single dataset and estimated the number of genetic clusters and Q-scores using STRUCTURE

with the same parameters as the analysis including only our collected samples. The maximum Q-scores of all the individuals included in the observed and simulated datasets were plotted to detect possible F1 hybrids and backcrosses.

Isolation with migration coalescent models

Isolation with migration coalescent models (Hey & Nielsen, 2004) were performed using IMa2 (Hey & Nielsen, 2007) to estimate migration rates, population sizes, and divergence times between species from individuals collected off Hiroshima. Pairwise comparisons were performed to ease the estimation of parameters. Preliminary analyses were performed to select adequate priors for long runs. The final priors used for migration rates (m), divergence time (t), and population mutation rate (q) were 10, 15.5, and 80, respectively. The performance of each analysis was evaluated by checking the swapping rates, autocorrelation values between the first and second sets of analysis, and trend-line points. Final runs were carried out with a burn-in of 200,000 steps, 2,000,000 steps of Markov Chain Monte Carlo, and saving 20,000 genealogies for each pairwise comparison. Analyses were performed with 40 chains and heating schemes ("-ha0.975 -hb0.75"), as suggested in the manual. Migration rates independent of mutation rate were estimated as the effective number of migrants per generation (2NM). In contrast, estimates of population size and divergence time were only inferred between species, given the absence of mutation rate estimates.

Results

Descriptive statistics from microsatellite loci

All loci were polymorphic in each species, with the number of alleles per locus ranging from six to 21 in *S. cheni*, six to 41 in *S. inermis*, and five to 70 in *S. ventricosus* (**Table 2**). The mean Ho values were 0.664, 0.725, and 0.726 for *S. cheni*, *S. inermis*, and *S. ventricosus*, respectively. The

303 mean value of He was 0.691 for *S. cheni*, 0.766 for *S. inermis*, and 0.754 for *S. ventricosus*.
304 Significant differences in allele distributions (**Fig.S1**) were detected in 9 out of 10 microsatellite
305 loci (*P* values < 0.005), with 23 out of 30 pairwise comparisons being statistically significant (*P*
306 values < 0.002). Significant deviations from HWE expectations were detected in six tests, three
307 of them occurring in the locus CGN1 (*P* values < 0.005) (**Table S2**). Only one out of 360
308 pairwise comparisons of loci (SSC23-Sebi2 in *S. inermis* from Hiroshima) showed significant
309 linkage disequilibrium (*P* value < 0.001).

310 **Outlier microsatellite loci**

311 Two out of the 10 loci (KSs7 and CGN1) were under putative divergent selection (alpha-KSs7 =
312 1.38, alpha-CGN1 = 1.50, adjusted *P* values using FDR < 0.002). In addition, Sebi2 presented
313 some signal of putative divergent selection (alpha = 0.89), but without statistical significance
314 (adjusted FDR *P* value < 0.09). The FST values among species calculated from these loci were
315 0.233 and 0.215 in CGN1 and KSs7, respectively, 0.15 in Sebi2, in contrast to a mean value of
316 0.06 in the other seven microsatellite loci (**Table S3**).

317 **Genetic clusters and individual admixture analysis**

318 The most likely number of genetic clusters was three as suggested by the Evanno Method (Δk =
319 795.07) (**Fig. S2**), clearly separating the three species (**Fig. 3**). However, clustering analyses
320 inferring four genetic clusters, separated the three species, and lumped RW and "Kumano"
321 specimens in a single cluster (**Fig. 3**). Meanwhile, clustering analyses excluding the two loci
322 under significant divergent selection, identified two clusters (Δk = 1224.42) (**Fig. S3**), which
323 only allowed the discrimination of *S. ventricosus* from the other two species (**Fig. 3**). Given that
324 we aimed to discriminate species and detect hybrids between them, we extended the explanation
325 of the results using all microsatellite loci. A total of 331 individuals were assigned as pure (Q >

0.90), and 29 as putative genetic hybrids. Among the BW individuals, two and 21 were genetically assigned to *S. cheni* and *S. ventricosus*, respectively. The RW group contained 20 and six individuals that genetically qualified as *S. cheni* and hybrids, respectively.

The distribution of maximum Q-scores from the simulated samples indicated that pure and F1 hybrids could be clearly discriminated; however, backcrosses presented overlapping Q-scores with pure and F1 hybrids (**Fig. 4**). Indeed, F1 hybrids presented maximum Q-scores ranging from 0.5 to 0.80, while backcrosses varied from 0.5 to 1 (**Fig. 4**).

Isolation with migration models

Statistically significant rates of introgression were detected from *S. ventricosus* to *S. cheni* (likelihood ratio test *P value* < 0.001, mean 2NM = 2.013, 95% highest posterior density (HPD) = 0.613–2.933) and from *S. inermis* to *S. ventricosus* (*P* value < 0.05, mean 2NM = 0.305, 95%HPD = 0.0425–1.379). The coalescent-based analysis suggested that the divergence between *S. cheni* and *S. ventricosus* occurred later (t0 = 0.329, 95% HPD = 0.10–0.63) than the divergence of the former and *S. inermis* (t0 = 0.669, 95% HPD = 0.147–1.294), and the split of *S. inermis* and *S. ventricosus* (t0 = 0.686, 95% HPD = 0.07–1.558). Population size estimations differed between species, with *S. cheni* presenting lower values (q = 3.372, 95% HPD = 1.64–5.24), followed by those of *S. ventricosus* (q = 4.815, 95% HPD = 2.2–7.96), and *S. inermis* (q = 5.946, 95% HPD = 2.92–9.40).

Species divergence inferred from microsatellite loci, D-loop and RH1 sequences

Genetic divergences between species were estimated only using specimens from Hiroshima presenting unequivocal morphology and non-admixed genetic ancestry in clustering analyses. Pairwise FST distances between species ranged from 0.11 (*S. cheni* vs. *S. inermis*) to 0.134 (*S. cheni* vs. *S. ventricosus*) (*P* values < 0.001) (**Table 3**). The D-loop alignment contained 616 bp

and was collapsed into 82 haplotypes. All three species and intermediate morphotypes presented haplotype and nucleotide diversity higher than 0.9 and 0.05, respectively (**Table S4**). D-loop haplotypes were not segregated in separate areas within the haplotype network, in agreement with the assignment of individuals to their respective origin within a species or putative hybrid group (**Fig. 5A**). However, all the pairwise K2P distances estimated from species and putative morphological hybrids were statistically significant (*P* values < 0.002) except for the comparison *S. ventricosus* and BW (**Table 3**). The shortest interspecific difference occurs between *S. inermis* and *S. ventricosus* (FST = 0.119) and the largest between *S. cheni* and *S. ventricosus* (FST = 0.358) (**Table 3**).

The 480bp-alignment of the RH1 gene, including samples from the three species, intermediate morphotypes, and genetically putative hybrids, was collapsed into four haplotypes. All *S. ventricosus* individuals were collapsed into a single haplotype (the main haplotype) highly present in the *S. inermis* (60 % of haploid sequences), BW (90%), RW (100%), and "Kumano" (50%) groups (**Fig. 5B**). Approximately 88% of *S. cheni* individuals had a haplotype differing from the main haplotype by one single mutational step, while 40% of *S. inermis* samples carried a different haplotype with variation in one mutation from the main one. The fourth haplotype was exclusively found in "Kumano" specimens and was derived from the *S. inermis* haplotype. The alignment of rhodopsin sequences including other *Sebastes* helped us to infer that the three species and the "Kumano" morphotype presented eight common amino acid replacements (*i.e.*, nonsynonymous mutations) at positions 119, 133, 158, 205, 213, 274, 277, and 286 of the rhodopsin protein, with two of them occurring only in this species complex (133 and 286) (**Table S5**). The mutations exclusively present in *S. cheni*, and some "Kumano" individuals were found to cause amino acid replacements in the positions 165 (from serine to alanine) and 217 (from

methionine to threonine) of the protein sequence, respectively. In contrast, the mutation observed in some *S. inermis* individuals did not change the amino acid sequence of the rhodopsin protein (*i.e.*, synonymous replacement).

Discussion

Divergences within the species complex

Kai & Nakabo (2008) proposed the splitting of *S. inermis* into three species based on differences in colouration, meristic counts, body proportions, and significant genetic divergences estimated from D-loop sequences and AFLP. Our findings support the significant genetic differences in the D-loop sequences of individuals occurring in sympatry and confirm them as genetically pure based on the Q-scores obtained from microsatellite loci. Although we did not use AFLP, the concomitant large genetic divergences estimated from D-loop sequences in both studies highlights the usefulness of these microsatellite loci as additional references for species identification. Moreover, the haplotype network aligns with the lack of reciprocal monophyly described by Kai, Nakayama & Nakabo (2002) in samples from the Seto Inland Sea, Noto (Ishikawa Prefecture), and Wakasa Bay (Kyoto Prefecture). The temporal and geographic extension of these interspecific differences highlights the spatio-temporal stability of the species boundaries delimitated through D-loop sequences, despite the likely incomplete lineage sorting or introgressive hybridization suggested by these authors and occurring in other closely related rockfishes (Hyde & Vetter, 2007; Schwenke, Park & Hauser, 2018). The large FST estimated from microsatellite loci are concordant with divergences between other rockfishes in large sympatry (Roques, Sévigny & Bernatchez, 2001; Narum et al., 2004). The existence of significantly different allele distributions between sympatric species (**Fig. S1**) and the genetic clusters inferred through STRUCTURE analysis in concordance with the taxonomic description

of the three species suggests that our dataset of microsatellite loci is sufficiently informative to separate them despite the confounding effect of high mutation rates and the multi-step mutation model of these markers, possibly leading to congruences in allele sizes (Estoup, Jarne & Cornuet, 2002; Morales et al., 2021).

The maximum absorption spectra (λ_{MAX}) of downwelling light among vertebrates is greatly determined by the type of chromophore bound to the opsin proteins, including RH1, as well as amino acid combinations at specific spectral tunning sites (Yokoyama & Takenaka, 2004). Changes in the amino acid composition of the RH1 protein can impact the visual sensitivity to dim light, as they alter the structural composition of the protein and, consequently, the absorption spectra (Bowmaker, 2008). Given the decreasing trend of downwelling light intensity along the water column, nonsynonymous mutations in RH1 suggest that species inhabit environments with different levels of downwelling light due to divergences in distribution depth (Jerlov, 1976). Our RH1 alignment including other *Sebastes* species revealed seven amino acid replacements at positions under positive selection (**Table S5**). These replacements coincidentally occurred in our focal species and other rockfishes inhabiting shallow environments (Sivasundar & Palumbi, 2010; Shum et al., 2014). For example, a replacement of isoleucine with leucine at position 119 of the RH1 protein has been associated with shifts into shallower environments (Sivasundar & Palumbi, 2010), with a punctual variation at this position occurring in the "deep" (isoleucine) and "shallow" (valine) groups within the beaked redfish *Sebastes mentella* Travin, 1951 (Shum et al., 2014).

The mutations identified in the RH1 gene of our focal species provide insights into their ecological differences in distribution, consistent with recent ecomorphological analyses (Deville et al., 2023). In the case of *S. inermis*, it shares the same amino acid sequence as *S. ventricosus*,

418 because the distinctive mutation found in the former does not cause an amino acid replacement
419 in the RH1 protein. Thus, the adaptations of *S. inermis* to deeper environments with lower light
420 intensity are likely manifested through other mechanisms, such as larger relative eye sizes
421 (Deville et al., 2023), which enable them to capture more photons (Warrant, 2000). The
422 congruence in amino acid sequences in both species may represent a common adaptation to
423 shallower environments with low light intensity, such as *Zostera L.* and *Sargassum* C. Agardh,
424 1820 beds, where *S. inermis* is usually found (Kai & Nakabo, 2008) and *S. ventricosus* can
425 occasionally incurs (Shoji et al., 2017). On the other hand, *S. cheni* exhibits a nonsynonymous
426 mutation that leads to an amino acid replacement from serine to alanine at position 165. This
427 nonsynonymous mutation has not been reported in any of the 35 *Sebastes* species with available
428 rhodopsin sequences but has been observed in certain cichlid with λ_{MAX} between 498 and 503
429 nm that inhabit rocky environments in shallow waters of the Tanganyika Lake (Sugawara et al.,
430 2005). Structural analysis of the rhodopsin protein has revealed that the position 165 is in the 4th
431 transmembrane domain (Palczewski et al., 2000; Sivasundar & Palumbi, 2010), with any amino
432 acid replacement at this position possibly altering the dimerization interface of the functional
433 protein, and thereby changing the λ_{MAX} (Schott et al., 2014; Ito et al., 2022). Thus, it is likely that
434 the amino acid replacement at position 165 position in *S. cheni* results in changes to its λ_{MAX} in
435 response to a different downwelling light intensities compared to the other two species. Although
436 the specific λ_{MAX} ranges for these species would provide a deeper understanding of their visual
437 adaptations to environments with dim light conditions (*e.g.*, Sugawara et al., 2005), the presence
438 of an amino acid replacement in *S. cheni* underscores the significance of selective pressures
439 driving ecological diversification within the species complex, supporting its previous split into
440 independent species.

Hybridization within the species complex

Hybridization was inferred from intermediate morphotypes, population genetic assessment, and coalescent analyses. Although the first method eased the identification of hybrids in the second method, it reduced the possibility of obtaining significant migration rates between species because putative morphological hybrids could not be assigned to any species in the coalescent analyses.

A total of 29 putative hybrids were detected in our population genetic surveys using clustering analyses with the full set of microsatellite loci. The performance of our STRUCTURE analysis to detect these hybrids relies on a confidence rate of 90%, because our number of loci, genetic divergences between the parent species (FST > 0.12), and the proportion of hybrids in the samples (~8.33%) are close to the ones necessary to attain this rate considering a Q-score threshold value of 0.9 to classify an individual as genetically putative pure or hybrid (Vähä & Primmer, 2006; Sanz et al., 2009). Based on Q-scores, 14 individuals were classified as putative genetic hybrids of *S. cheni – S. ventricosus*, 13 as *S. cheni – S. inermis*, and 2 as *S. inermis – S. ventricosus* hybrids. However, it is important to note that the percentage of hybrids inferred from clustering analyses may be underestimated, as some genetically pure individuals with intermediate morphotypes may be backcrosses, as indicated by our simulations (**Fig. 4**). Considering this, a total of 50 potential backcrosses could be inferred in our samples.

Migration estimates from coalescent models only indicate significant asymmetric rates of migration from *S. ventricosus* to *S. cheni*, and from *S. inermis* to *S. ventricosus*. The lack of significance in the highest migration rate between *S. cheni* and *S. inermis*, estimated as 2NM = 0.763 (95% HPD = 0–1.607) from the latter to the former, is due to the exclusion of intermediate morphotypes in the coalescent models. Additionally, the inclusion of two loci under divergent

selection (KSs7 and CGN1) that allow discrimination of *S. cheni* and *S. inermis,* may lead to lower estimates of migration rates as introgression of alleles at these loci is reduced between species, resulting in an overall reduction in migration rate estimates (Feder, Egan & Nosil, 2012). These asymmetric migration rates align with theoretical expectations, where smaller populations receive introgression from larger populations over time (Arnold, Hamrick & Bennett, 1993). Therefore, introgression of new alleles from the other species counteracts the lower genetic diversity observed in *S. cheni* (**Tables 2 and S3**), which may be attributed to a stronger effect of genetic drift resulting from its smaller effective population sizes (Allendorf, 1986).

Putative morphological hybrids exhibit intermediate colouration and meristic patterns, but with otolith weight ~ age relationships resembling *S. cheni*. The presence of intermediate color polymorphisms, along with hybridization events, suggests that coloration patterns alone may not be sufficient for maintaining reproductive isolation between species (Gray & McKinnon, 2007). It is possible that other factors, such as specific environmental conditions and assortative mating, play a role in determining the relevance of coloration patterns for reproductive isolation (Fuller, Houle & Travis, 2005).

Introgression driven by females is expected to occur in this species complex because females approach the male territories during reproductive seasons and can decide whether to initiate copulation (Shinomiya & Ezaki, 1991). The network of D-loop haplotypes did not show any shared haplotype between either intermediate morphotypes or putative genetic hybrids and any species, indicating no evidence of introgression driven by females. However, several factors suggest that intermediate morphotypes, specifically the BW, RW, and “Kumano” morphotypes, are more likely to have originated from mating pairs where a male *S. cheni* mated with a female *S. ventricosus* (BW morphotype) or *S. inermis* (RW and “Kumano” morphotypes). These mating

pairs are supported through the larger genetic divergences between intermediate morphotypes and *S. cheni* (**Table 3**), along with the otolith weight ~ age relationships of intermediate morphotypes resembling those of *S. cheni* (**Fig. 2**), and *in situ* observations indicating that females tend to copulate with males larger than them (Shinomiya & Ezaki, 1991). These types of mating pairs might occur since at same ages *S. cheni* males attain larger sizes than males from the other two species, and males are larger than females, except for *S. ventricosus* (Kamimura et al., 2014). This size difference may provide a selective advantage during reproductive seasons, as larger males establish larger territories, engage in agonistic behaviours, patrol their territories, and perform courtship when encountering females (Shinomiya & Ezaki, 1991). On the other hand, smaller males have smaller territories, do not exhibit agonistic behaviour, and do not perform courtship (Shinomiya & Ezaki, 1991). Hence, the hypothesis that introgression occurs through females in this species complex is supported by a relative higher fitness of *S. cheni*, BW, RW, and "Kumano" males during reproductive seasons due to their larger size and the size-assortative mating behaviour driven by females.

All genetically putative hybrids detected in individuals with intermediate morphotypes exhibited the same RH1 haplotype as *S. ventricosus*. This observation may indicate introgression of RH1 haplotypes between species with positive frequency-dependent selection in favour of the haplotype present in *S. ventricosus* (Sinervo & Calsbeek, 2006). Considering that hybridization is mediated by females and that the two RW intermediate morphotypes slightly differing in colouration (**Fig. 2**) were only found in two specific sampling sites (Osaki-Shimozima East and Etajima Islands) off Hiroshima, this selection process may be particularly influential in the perception of male coloration by females in dim light environments (Fuller, Houle & Travis, 2005), such as seagrass beds where *S. inermis* and *S. cheni* engage in foraging activities (Shoji et

al., 2017). In these environments, the persistence of intermediate colour morphotypes in RW individuals is not only explained through the synergy of size-assortative mating and colour preferences of females, but also through their higher fitness at foraging and performing defensive responses against predators, since a red-brown colouration may provide camouflage within seagrass beds, making it more difficult to detect compared to the red coloration of *S. inermis* against the seagrass background (Fuller, Houle & Travis, 2005; Deville et al., 2023).

Despite the advantages conferred by assortative mating and selective traits of RW hybrids in specific environments, hybridization rates can be reduced due to polygamy (Shinomiya & Ezaki, 1991). Females generally can mate with males of the same species, limiting interbreeding to special circumstances. The selective advantage of other hybrids, along with assortative mating, and polygamy, can also explain the lack of intermediate morphotypes between *S. inermis* and *S. ventricosus* with lower growth rates and potential fitness disadvantages, which can be contributing to the reproductive isolation between these species (*i.e.*, reinforcement) (Dobzhansky, 1940; Servedio & Noor, 2003). Furthermore, considering the increased probability of hybridization events due to stock enhancement programmes releasing thousands of juveniles from the three species along the coastal waters of Japan (Nakagawa, 2008), assortative mating, polygamy, and reinforcement gain significance in maintaining species integrity and preventing further hybridization.

Speciation-with-gene-flow in the species complex

The patterns of hybridization observed in these rockfish species provide strong evidence for the semipermeable nature of their species boundaries (Harrison & Larson, 2014), indicating that they fall into the second and third stages of speciation described by Wu (2001). In these stages, introgression can only occur in genomic regions not crucial for maintaining species boundaries,

parent species can hybridize forming hybrid swarms consisting of fertile hybrids with intermediate morphotypes (Mayr, 1963; Wu, 2001), and their independent evolution in sympatry is maintained through competitive exclusion (Wu, 2001; Deville et al., 2023). The occurrence of two loci under putative directional selection (KSs7 and CGN1, **Table S3**), with "outlier" high FST values along with hybrids and independent divergence of each species support the scenario of speciation-with-gene-flow whereby these two loci are linked to genomic regions of divergence, which contain genes crucial for maintaining species boundaries that may not be exchanged during hybridization (Nosil, Funk & Ortiz-Barrientos, 2009).

In a scenario of speciation-with-gene-flow, species divergence is greatly driven by divergent selection related to specific habitats or environments (Feder, Egan & Nosil, 2012), as supported by their ecomorphological divergences in sympatry (Deville et al., 2023). The anomalously high interspecific divergence in loci under putative directional selection (FST > 0.21), along with low diversity values within each species and deviations from the HWE (especially in the CGN1 locus) (**Table S2**), further support the occurrence of a purely ecological selective sweep (Schlötterer 2002, 2003; Buonaccorsi et al. 2011). This type of selective sweep occurs when a genomic region's variation is reduced or eliminated due to its proximity to a new beneficial mutation that is increasing in frequency through recent adaptation (Hermisson & Pennings, 2017). Other findings suggestive of an ecologically selective sweep are the absence of FST outliers in KSs7 scored in other rockfishes inhabiting the same area, which are genetically close to the *S. inermis* species complex (An et al., 2009), since new advantageous mutations causing adaptive divergence and linked to the KSs7 loci might have appeared more recently. Similar cases of selective sweeps have been observed in closely related rockfishes occupying different depths (Buonaccorsi et al., 2011; Behrens et al., 2021; Olivares-Zambrano et al., 2022) and in

depth-related ecotypes within the same species (Saha et al., 2021). The occurrence of ecologically selective sweeps across *Sebastes* rockfishes indicates that recent adaptation to new environments is contributing to the ongoing diversification of species. Therefore, further characterization of the genomic variation surrounding the KSs7 and CGN1 loci is necessary to determine the conditions that promote diversification within the *S. inermis* complex.

The "Kumano" morphotype

The "Kumano" specimens exhibit a brown-red colouration and meristic patterns that overlap between *S. cheni* and *S. inermis*, but their otolith weight ~ age relationships are more similar to *S. cheni* (**Fig. 2**). This combination of morphological features explains why local fishermen consider this morphotype as a "big variant" of the red-coloured rockfish *S. inermis*. Although genetic divergences were not estimated due to the low number of individuals, the D-loop haplotypes indicate that the "Kumano" specimens are part of the species complex. Analysis of the Seb1 locus, used by Deville et al. (2023) to discriminate *S. ventricosus*, suggests that this morphotype does not possess the typical alleles of *S. ventricosus* (>160 bp) (**Fig. S1**). In terms of the two loci under putative directional selection, the "Kumano" specimens carry the most frequent allele of *S. inermis* in the CGN1 locus and some exclusive alleles in the KSs7 locus (**Fig. S1**). STRUCTURE analysis suggests a possible hybrid origin for the "Kumano" specimens, with approximately 75-82% of their ancestry corresponding to *S. inermis*, along with fractions of 10-16% *S. cheni* in three individuals, and 16% *S. ventricosus* in one specimen. However, when four genetic clusters were inferred using STRUCTURE analysis, "Kumano" specimens and the RW morphotype were grouped together in a separate category with high Q-scores (**Fig. 2**). Additionally, a punctual amino acid replacement was observed at position 217 in some individuals, causing an amino acid replacement from threonine to methionine across the three

579 species of the complex (**Table S5**). This amino acid replacement has been associated with shifts
580 into shallower waters in other rockfishes (Sivasundar & Palumbi, 2010). The position 217 falls
581 under the 5th transmembrane domain, and possible changes in this position are related to
582 modifications in the λ_{MAX}, which relates to visual sensitivity (Schott et al., 2014). These findings
583 suggest that the endemic "Kumano" morphotype might present exclusive alleles in loci
584 responsible for maintaining species divergence in the presence of sympatry and gene flow within
585 the species complex. Considering this evidence, a hypothetical hybrid origin of this morphotype
586 aligns with theoretical models predicting that introgression, combined with intermediate
587 assortative mating and low variation in reproductive success, can act as a potential mechanism
588 for rapid evolution in specific environments (Baskett & Gomulkiewicz, 2011). The first
589 condition, intermediate assortative mating, is fulfilled in this species complex, while the second
590 depends on the level of preference of females for the "Kumano" morphotype, which is
591 considered "rare". A comprehensive morphological and genetic characterization of more
592 individuals is necessary to assess this hypothetical hybrid origin and support the emergence of
593 "Kumano" as an incipient species resulting from the ongoing process of speciation-with-gene-
594 flow within the *S. inermis* complex.

595 ## Conclusions
596

597 The dynamics of introgression and genetic divergences was assessed within the *Sebastes inermis*
598 (*Sebastes cheni*, viz *Sebastes inermis*, *Sebastes ventricosus*, and their putative morphological
599 hybrids) by using sequences of the mitochondrial control region (D-loop), the intron-free
600 rhodopsin (RH1) gene, and 10 microsatellite loci. We hypothesize that each species would
601 maintain its genetic divergence even in the presence of introgression, and that putative
602 morphological hybrids would exhibit genetic admixed ancestry of the parent species. We found

large genetic divergences in D-loop, along with mutations in the RH1 gene, and three genetic clusters obtained from microsatellite loci, that are concordant with the morphological description of each species. Of the three species, *S. cheni* is the unique with a nonsynonymous mutation in the RH1 gene, which suggest differential adaptations of this species to dim light conditions. Introgression was confirmed through significant migration rates between species and admixed genetic ancestry. Two microsatellite loci under divergent selection suggest that they are possibly linked to genomic regions whereby interspecific gene flow is typically restricted because they are crucial for maintain species boundaries. A further characterization of genomic regions surrounding these loci is pending. Additionally, the genetic admixed ancestry, nonsynonymous mutation in the RH1 gene, and exclusive alleles in loci under divergent selection within one putative morphological hybrid known as “Kumano”, along with the independent divergence of each species point out the potential role of introgression regarding speciation within the *Sebastes inermis* complex. Our findings urge the need for further studies aimed to assess the relative fitness of hybrids and parentals in sympatry, specifically in the context of stock enhancement programmes, which can potentially increase chances of introgression within the species complex.

Acknowledgements

We would like to thank all lab members, and Gou Uehara and Shunji Uehara, who kindly provided samples and helped with logistical support to ease the collection of specimens. We thank Hirosuke Kimura, Naoyuki Nakase, and Ph.D. Keisuke Doi for generously providing us with the "Kumano" samples to help uncover the identity of this unique morphotype.

References

1. Abbott R, Albach D, Ansell S, Arntzen JW, Baird SJE, Bierne N, Boughman J, Brelsford A, Buerkle CA, Buggs R, Butlin RK, Dieckmann U, Eroukhmanoff F, Grill A, Cahan SH, Hermansen JS, Hewitt G, Hudson AG, Jiggins C, Jones J, Keller B, Marczewski T, Mallet J, Martinez-Rodriguez P, Möst M, Mullen S, Nichols R, Nolte AW, Parisod C, Pfennig K, Rice AM, Ritchie MG, Seifert B, Smadja CM, Stelkens R, Szymura JM, Väinölä R, Wolf JBW, Zinner D. 2013. Hybridization and speciation. *Journal of Evolutionary Biology* **26**:229–246 DOI: 10.1111/j.1420-9101.2012.02599.x.
2. Allendorf FW. 1986. Genetic drift and the loss of alleles versus heterozygosity. *Zoo Biology* **5**:181–190 DOI: 10.1002/zoo.1430050212.
3. An HS, Park JY, Kim M-J, Lee EY, Kim KK. 2009. Isolation and characterization of microsatellite markers for the heavily exploited rockfish *Sebastes schlegeli,* and cross-species amplification in four related *Sebastes* spp. *Conservation Genetics* **10**:1969 DOI: 10.1007/s10592-009-9870-8.
4. Anderson E. 1949. Introgressive hybridization. New York: Wiley & Sons.
5. Arnold ML. 1992. Natural Hybridization as an Evolutionary Process. *Annual Review of Ecology and Systematics* **23**:237–261 DOI: 10.1146/annurev.es.23.110192.001321.
6. Arnold ML, Fogarty ND. 2009. Reticulate Evolution and Marine Organisms: The Final Frontier? *International Journal of Molecular Sciences* **10**:3836–3860. DOI 10.3390/ijms10093836.
7. Arnold ML, Hamrick JL, Bennett BD. 1993. Interspecific Pollen Competition and Reproductive Isolation in Iris. *Journal of Heredity* **84**:13–16. DOI 10.1093/oxfordjournals.jhered.a111269.

649 8. Artamonova VS, Makhrov AA, Karabanov DP, Rolskiy AYu, Bakay YuI, Popov VI. 2013.
650 Hybridization of beaked redfish (*Sebastes mentella*) with small redfish (*Sebastes viviparus*)
651 and diversification of redfish (Actinopterygii: Scorpaeniformes) in the Irminger Sea. *Journal*
652 *of Natural History* **47**:1791–1801. DOI 10.1080/00222933.2012.752539.
653 9. Asahida T, Kobayashi T, Saitoh K, Nakayama I. 1996. Tissue preservation and total DNA
654 extraction form fish stored at ambient temperature using buffers containing high
655 concentration of urea. *Fisheries science* **62**:727–730. DOI 10.2331/fishsci.62.727.
656 10. Baskett ML, Gomulkiewicz R. 2011. Introgressive hybridization as a mechanism for species
657 rescue. *Theoretical Ecology* **4**:223–239. DOI 10.1007/s12080-011-0118-0.
658 11. Beaumont MA, Balding DJ. 2004. Identifying adaptive genetic divergence among
659 populations from genome scans. *Molecular Ecology* **13**:969–980. DOI 10.1111/j.1365-
660 294X.2004.02125.x.
661 12. Behrens KA, Girasek QL, Sickler A, Hyde J, Buonaccorsi VP. 2021. Regions of genetic
662 divergence in depth-separated *Sebastes* rockfish species pairs: Depth as a potential driver of
663 speciation. *Molecular Ecology* **30**:4259–4275. DOI 10.1111/mec.16046.
664 13. Benjamini Y, Hochberg Y. 1995. Controlling the False Discovery Rate: A Practical and
665 Powerful Approach to Multiple Testing. *Journal of the Royal Statistical Society Series B*
666 *(Methodological)* **57**:289–300.
667 14. Berntson EA, Moran P. 2009. The utility and limitations of genetic data for stock
668 identification and management of North Pacific rockfish (*Sebastes* spp.). *Review in Fish*
669 *Biology and Fisheries* **19**:233–247. DOI 10.1007/s11160-008-9101-2.
670 15. Blacket MJ, Robin C, Good RT, Lee SF, Miller AD. 2012. Universal primers for fluorescent
671 labelling of PCR fragments—an efficient and cost-effective approach to genotyping by

672 fluorescence. *Molecular Ecology Resources* **12**:456–463. DOI 10.1111/j.1755-
673 0998.2011.03104.x.
674 16. Blanco Gonzalez E, Murakami T, Teshima Y, Yoshioka K, Jeong D-S, Umino T. 2009.
675 Paternity testing of wild black rockfish *Sebastes inermis* (brownish type) from the Seto
676 Inland Sea of Japan. *Ichthyological Research* **56**:87–91. DOI 10.1007/s10228-008-0055-0.
677 17. Bowmaker JK. 2008. Evolution of vertebrate visual pigments. *Vision Research* **48**:2022–
678 2041. DOI 10.1016/j.visres.2008.03.025.
679 18. Buonaccorsi VP, Kimbrell CA, Lynn EA, Vetter RD. 2005. Limited realized dispersal and
680 introgressive hybridization influence genetic structure and conservation strategies for brown
681 rockfish, *Sebastes auriculatus*. *Conservation genetics* **6**:697–713. DOI 10.1007/s10592-005-
682 9029-1.
683 19. Buonaccorsi VP, Narum SR, Karkoska KA, Gregory S, Deptola T, Weimer AB. 2011.
684 Characterization of a genomic divergence island between black-and-yellow and gopher
685 *Sebastes* rockfishes. *Molecular Ecology* **20**:2603–2618. DOI 10.1111/j.1365-
686 294X.2011.05119.x.
687 20. Burford MO. 2009. Demographic history, geographical distribution and reproductive
688 isolation of distinct lineages of blue rockfish (*Sebastes mystinus*), a marine fish with a high
689 dispersal potential. *Journal of Evolutionary Biology* **22**:1471–1486. DOI 10.1111/j.1420-
690 9101.2009.01760.x.
691 21. Chen W-J, Bonillo C, Lecointre G. 2003. Repeatability of clades as a criterion of reliability:
692 a case study for molecular phylogeny of Acanthomorpha (Teleostei) with larger number of
693 taxa. *Molecular Phylogenetics and Evolution* **26**:262–288. DOI 10.1016/S1055-
694 7903(02)00371-8.

22. Clement M, Posada D, Crandall KA. 2000. TCS: a computer program to estimate gene genealogies. *Molecular Ecology* **9**:1657–1659. DOI 10.1046/j.1365-294x.2000.01020.x.

23. Corander J, Marttinen P, Sirén J, Tang J. 2008. Enhanced Bayesian modelling in BAPS software for learning genetic structures of populations. *BMC Bioinformatics* **9**:539. DOI 10.1186/1471-2105-9-539.

24. Deville D, Sanchez G, Barahona SP, Yamashiro C, Oré-Chávez D, Bazán RQ, Umino T. 2021. Spatio-temporal patterns of genetic variation of the silverside *Odontesthes regia* in the highly productive Humboldt Current System. *Fisheries Research* **244**:106127. DOI 10.1016/j.fishres.2021.106127.

25. Deville D, Kawai K, Fujita H, Umino T. 2023. Ecomorphology of three closely related *Sebastes* rockfishes with sympatric occurrence in Seto Inland Sea, Japan. *Hydrobiologia*. DOI 10.1007/s10750-023-05286-4.

26. Dobzhansky T. 1940. Speciation as a stage in evolutionary divergence. *The American Naturalist* **74**: 302–321.

27. Earl DA, vonHoldt BM. 2012. STRUCTURE HARVESTER: a website and program for visualizing STRUCTURE output and implementing the Evanno method. *Conservation Genetics Resources* **4**:359–361. DOI 10.1007/s12686-011-9548-7.

28. Estoup A, Jarne P, Cornuet J-M. 2002. Homoplasy and mutation model at microsatellite loci and their consequences for population genetics analysis. *Molecular Ecology* **11**:1591–1604. DOI 10.1046/j.1365-294X.2002.01576.x.

29. Evanno G, Regnaut S, Goudet J. 2005. Detecting the number of clusters of individuals using the software structure: a simulation study. *Molecular Ecology* **14**:2611–2620. DOI 10.1111/j.1365-294X.2005.02553.x.

718 30. Excoffier L, Lischer HEL. 2010. Arlequin suite ver 3.5: a new series of programs to perform
719 population genetics analyses under Linux and Windows. *Molecular Ecology Resources*
720 **10**:564–567. DOI 10.1111/j.1755-0998.2010.02847.x.
721 31. Feder JL, Egan SP, Nosil P. 2012. The genomics of speciation-with-gene-flow. *Trends in*
722 *Genetics* **28**:342–350. DOI 10.1016/j.tig.2012.03.009.
723 32. Foll M, Gaggiotti O. 2008. A Genome-Scan Method to Identify Selected Loci Appropriate
724 for Both Dominant and Codominant Markers: A Bayesian Perspective. *Genetics* **180**:977–
725 993. DOI 10.1534/genetics.108.092221.
726 33. Fuller RC, Houle D, Travis J. 2005. Sensory Bias as an Explanation for the Evolution of
727 Mate Preferences. *The American Naturalist* **166**:437–446. DOI 10.1086/444443.
728 34. Gao T, Ding K, Song N, Zhang X, Han Z. 2018. Comparative analysis of multiple paternity
729 in different populations of viviparous black rockfish, *Sebastes schlegelii*, a fish with long-
730 term female sperm storage. *Marine Biodiversity* **48**:2017–2024. DOI 10.1007/s12526-017-
731 0713-4.
732 35. Gray SM, McKinnon JS. 2007. Linking color polymorphism maintenance and speciation.
733 *Trends in Ecology & Evolution* **22**:71–79. DOI 10.1016/j.tree.2006.10.005.
734 36. Harrison RG, Larson EL. 2014. Hybridization, Introgression, and the Nature of Species
735 Boundaries. *Journal of Heredity* **105**:795–809. DOI 10.1093/jhered/esu033.
736 37. Hermisson J, Pennings PS. 2017. Soft sweeps and beyond: understanding the patterns and
737 probabilities of selection footprints under rapid adaptation. *Methods in Ecology and*
738 *Evolution* **8**:700–716. DOI 10.1111/2041-210X.12808.

739 38. Hey J, Nielsen R. 2004. Multilocus methods for estimating population sizes, migration rates
740 and divergence time, with applications to the divergence of *Drosophila pseudoobscura* and
741 *D. persimilis*. *Genetics* **167**:747–760. DOI 10.1534/genetics.103.024182.
742 39. Hey J, Nielsen R. 2007. Integration within the Felsenstein equation for improved Markov
743 chain Monte Carlo methods in population genetics. *Proceedings of the National Academy of*
744 *Sciences* **104**:2785–2790. DOI 10.1073/pnas.0611164104.
745 40. Hyde JR, Vetter RD. 2007. The origin, evolution, and diversification of rockfishes of the
746 genus *Sebastes* (Cuvier). *Molecular Phylogenetics and Evolution* **44**:790–811. DOI
747 10.1016/j.ympev.2006.12.026.
748 41. Ito RK, Harada S, Tabata R, Watanabe K. 2022. Molecular evolution and convergence of the
749 rhodopsin gene in *Gymnogobius*, a goby group having diverged into coastal to freshwater
750 habitats. *Journal of Evolutionary Biology* **35**:333–346. DOI 10.1111/jeb.13955.
751 42. Jerlov NG. 1976. Marine optics. Amsterdam, The Netherlands: Elsevier.
752 43. Kai Y, Nakabo T. 2008. Taxonomic review of the *Sebastes inermis* species complex
753 (Scorpaeniformes: Scorpaenidae). *Ichthyological Research* **55**:238–259. DOI
754 10.1007/s10228-007-0029-7.
755 44. Kai Y, Nakayama K, Nakabo T. 2002. Genetic differences among three colour morphotypes
756 of the black rockfish, *Sebastes inermis*, inferred from mtDNA and AFLP analyses. *Molecular*
757 *Ecology* **11**:2591–2598. DOI 10.1046/j.1365-294x.2002.01628.x.
758 45. Kamimura Y, Kawane M, Hamaguchi M, Shoji J. 2014. Age and growth of three rockfish
759 species, *Sebastes inermis*, *S. ventricosus* and *S. cheni* , in the central Seto Inland Sea, Japan.
760 *Ichthyological Research* **61**:108–114. DOI 10.1007/s10228-013-0381-8.

761 46. Kimura M. 1980. A simple method for estimating evolutionary rates of base substitutions
762 through comparative studies of nucleotide sequences. *Journal of Molecular Evolution*
763 16:111–120. DOI 10.1007/BF01731581.
764 47. Larkin MA, Blackshields G, Brown NP, Chenna R, McGettigan PA, McWilliam H, Valentin
765 F, Wallace IM, Wilm A, Lopez R, Thompson JD, Gibson TJ, Higgins DG. 2007. Clustal W
766 and Clustal X version 2.0. *Bioinformatics* **23**:2947–2948. DOI
767 10.1093/bioinformatics/btm404.
768 48. Leigh JW, Bryant D. 2015. popart: full-feature software for haplotype network construction.
769 *Methods in Ecology and Evolution* **6**:1110–1116. DOI 10.1111/2041-210X.12410.
770 49. Mayr E. 1963. Animal Species and Evolution. The Belknap press, Cambridge, MA.
771 50. Morales AE, Fenton MB, Carstens BC, Simmons NB. 2021. Comment on "Population
772 genetics reveal *Myotis keenii* (Keen's myotis) and *Myotis evotis* (long-eared myotis) to be a
773 single species." *Canadian Journal of Zoology* **99**:415–422. DOI 10.1139/cjz-2020-0048.
774 51. Muto N, Kai Y, Noda T, Nakabo T. 2013. Extensive hybridization and associated geographic
775 trends between two rockfishes *Sebastes vulpes* and *S. zonatus* (Teleostei: Scorpaeniformes:
776 Sebastidae). *Journal of Evolutionary Biology* **26**:1750–1762. DOI 10.1111/jeb.12175.
777 52. Nakagawa M. 2008. Studies of stock enhancement technology of the black rockfish *Sebastes*
778 *schlegeli. Bulletin of Fisheries Research Agency*. ISSN: 1346–9894.
779 53. Narum SR, Buonaccorsi VP, Kimbrell CA, Vetter RD. 2004. Genetic divergence between
780 gopher rockfish (*Sebastes carnatus*) and black and yellow rockfish (*Sebastes chrysomelas*).
781 *Copeia* **2004**:926–931.

782 54. Nielsen EE, Bach LA, Kotlicki P. 2006. hybridlab (version 1.0): a program for generating
783 simulated hybrids from population samples. *Molecular Ecology Notes* **6**:971–973. DOI
784 10.1111/j.1471-8286.2006.01433.x.
785 55. Nosil P, Funk DJ, Ortiz-Barrientos D. 2009. Divergent selection and heterogeneous genomic
786 divergence. *Molecular Ecology* **18**:375–402. DOI 10.1111/j.1365-294X.2008.03946.x.
787 56. Olivares-Zambrano D, Daane J, Hyde J, Sandel MW, Aguilar A. 2022. Speciation genomics
788 and the role of depth in the divergence of rockfishes (*Sebastes*) revealed through Pool-seq
789 analysis of enriched sequences. *Ecology and Evolution* 12:e9341. DOI 10.1002/ece3.9341.
790 57. Palczewski K, Kumasaka T, Hori T, Behnke CA, Motoshima H, Fox BA, Trong IL, Teller
791 DC, Okada T, Stenkamp RE, Yamamoto M, Miyano M. 2000. Crystal Structure of
792 Rhodopsin: A G Protein-Coupled Receptor. *Science* **289**:739–745. DOI
793 10.1126/science.289.5480.739.
794 58. Pritchard JK, Stephens M, Donnelly P. 2000. Inference of population structure using
795 multilocus genotype data. *Genetics* **155**:945–959.
796 59. Roques Sé, SÉvigny J-M, Bernatchez L. 2001. Evidence for broadscale introgressive
797 hybridization between two redfish (genus *Sebastes*) in the North-west Atlantic: a rare marine
798 example. *Molecular Ecology* **10**:149–165. DOI 10.1046/j.1365-294X.2001.01195.x.
799 60. Rozas J, Ferrer-Mata A, Sánchez-DelBarrio JC, Guirao-Rico S, Librado P, Ramos-Onsins
800 SE, Sánchez-Gracia A. 2017. DnaSP 6: DNA Sequence Polymorphism Analysis of Large
801 Data Sets. *Molecular Biology and Evolution* **34**:3299–3302. DOI 10.1093/molbev/msx248.
802 61. Saha A, Johansen T, Hedeholm R, Nielsen EE, Westgaard J-I, Hauser L, Planque B, Cadrin
803 SX, Boje J. 2017. Geographic extent of introgression in *Sebastes mentella* and its effect on
804 genetic population structure. *Evolutionary Applications* **10**:77–90. DOI 10.1111/eva.12429.

805 62. Saha A, Kent M, Hauser L, Drinan DP, Nielsen EE, Westgaard J-I, Lien S, Johansen T.
806 2021. Hierarchical genetic structure in an evolving species complex: Insights from genome
807 wide ddRAD data in *Sebastes mentella*. *PLOS ONE* **16**:e0251976. DOI
808 10.1371/journal.pone.0251976.
809 63. Sanz N, Araguas RM, Fernández R, Vera M, García-Marín J-L. 2009. Efficiency of markers
810 and methods for detecting hybrids and introgression in stocked populations. *Conservation*
811 *Genetics* **10**:225–236. DOI 10.1007/s10592-008-9550-0.
812 64. Schlötterer C. 2002. A microsatellite-based multilocus screen for the identification of local
813 selective sweeps. *Genetics* **160**:753–763.
814 65. Schlötterer C. 2003. Hitchhiking mapping – functional genomics from the population
815 genetics perspective. *Trends in Genetics* **19**:32–38. DOI 10.1016/S0168-9525(02)00012-4.
816 66. Schott RK, Refvik SP, Hauser FE, López-Fernández H, Chang BSW. 2014. Divergent
817 positive selection in rhodopsin from lake and riverine cichlid fishes. *Molecular Biology and*
818 *Evolution* **31**:1149–1165. DOI 10.1093/molbev/msu064.
819 67. Schwenke PL, Park LK, Hauser L. 2018. Introgression among three rockfish species
820 (*Sebastes* spp.) in the Salish Sea, northeast Pacific Ocean. *PLOS ONE* **13**:e0194068. DOI
821 10.1371/journal.pone.0194068.
822 68. Servedio MR, Noor MAF. 2003. The Role of Reinforcement in Speciation: Theory and Data.
823 *Annual Review of Ecology, Evolution, and Systematics* **34**:339–364.
824 69. Shaw KL, Mullen SP. 2011. Genes versus phenotypes in the study of speciation. *Genetica*
825 139:649–661. DOI 10.1007/s10709-011-9562-4.

826 70. Shinomiya A, Ezaki O. 1991. Mating habits of the rockfish *Sebastes inermis*. In: Boehlert
827 GW, Yamada J (eds) Rockfishes of the genus *Sebastes*: Their reproduction and early life
828 history. Springer Netherlands, Dordrecht, pp 15–22. DOI 10.1007/978-94-011-3792-8_2.
829 71. Shoji J, Mitamura H, Ichikawa K, Kinoshita H, Arai N. 2017. Increase in predation risk and
830 trophic level induced by nocturnal visits of piscivorous fishes in a temperate seagrass bed.
831 *Scientific Reports* **7**:3895. DOI 10.1038/s41598-017-04217-3.
832 72. Shum P, Pampoulie C, Sacchi C, Mariani S. 2014. Divergence by depth in an oceanic fish.
833 *PeerJ* **2**:e525. DOI 10.7717/peerj.525.
834 73. Sinervo B, Calsbeek R. 2006. The Developmental, Physiological, Neural, and Genetical
835 Causes and Consequences of Frequency-Dependent Selection in the Wild. *Annual Review of*
836 *Ecology, Evolution, and Systematics* **37**:581–610. DOI
837 10.1146/annurev.ecolsys.37.091305.110128.
838 74. Sivasundar A, Palumbi SR. 2010. Parallel amino acid replacements in the rhodopsins of the
839 rockfishes (*Sebastes* spp.) associated with shifts in habitat depth. *Journal of Evolutionary*
840 *Biology* **23**:1159–1169. DOI 10.1111/j.1420-9101.2010.01977.x.
841 75. Sugawara T, Terai Y, Imai H, Turner GF, Koblmüller S, Sturmbauer C, Shichida Y, Okada
842 N. 2005. Parallelism of amino acid changes at the RH1 affecting spectral sensitivity among
843 deep-water cichlids from Lakes Tanganyika and Malawi. *Proceedings of the National*
844 *Academy of Sciences* **102**:5448–5453. DOI 10.1073/pnas.0405302102.
845 76. Vähä J-P, Primmer CR. 2006. Efficiency of model-based Bayesian methods for detecting
846 hybrid individuals under different hybridization scenarios and with different numbers of loci.
847 *Molecular Ecology* **15**:63–72. DOI 10.1111/j.1365-294X.2005.02773.x.

848 77. Valentin A, Sévigny J-M, Chanut J-P. 2002. Geometric morphometrics reveals body shape
849 differences between sympatric redfish *Sebastes mentella*, *Sebastes fasdatus* and their hybrids
850 in the Gulf of St Lawrence. *Journal of Fish Biology* **60**:857–875. DOI 10.1111/j.1095-
851 8649.2002.tb02414.x.
852 78. Via S. 2001. Sympatric speciation in animals: the ugly duckling grows up. *Trends in Ecology*
853 *& Evolution* **16**:381–390. DOI 10.1016/S0169-5347(01)02188-7.
854 79. Warrant E. 2000. The eyes of deep-sea fishes and the changing nature of visual scenes with
855 depth. *Philosophical Transactions of the Royal Society B: Biological Sciences* **355**:1155–
856 1159.
857 80. Weir BS, Cockerham CC. 1984. Estimating F-Statistics for the Analysis of Population
858 Structure. *Evolution* **38**:1358–1370. DOI 10.2307/2408641.
859 81. Westerman ME, Buonaccorsi VP, Stannard JA, Galver L, Taylor C, Lynn EA, Kimbrell CA,
860 Vetter RD. 2005. Cloning and characterization of novel microsatellite DNA markers for the
861 grass rockfish, *Sebastes rastrelliger*, and cross-species amplification in 10 related *Sebastes*
862 spp. *Molecular Ecology Notes* **5**:74–76. DOI 10.1111/j.1471-8286.2004.00837.x.
863 82. Wu C-I. 2001. The genic view of the process of speciation. *Journal of Evolutionary Biology*
864 **14**:851–865. DOI 10.1046/j.1420-9101.2001.00335.x.
865 83. Yokoyama S, Takenaka N. 2004. The Molecular Basis of Adaptive Evolution of Squirrelfish
866 Rhodopsins. *Molecular Biology and Evolution* **21**:2071–2078. DOI 10.1093/molbev/msh217.
867 84. Yoshida K, Nakagawa M, Wada S. 2005. Multiplex PCR system applied for analysing
868 microsatellite loci of Schlegel's black rockfish, *Sebastes schlegeli. Molecular Ecology Notes*
869 **5**:416–418. DOI 10.1111/j.1471-8286.2005.00945.x.

870

Figure 1

Sampling sites along coastal waters of Japan. Black points represent sampling sites.

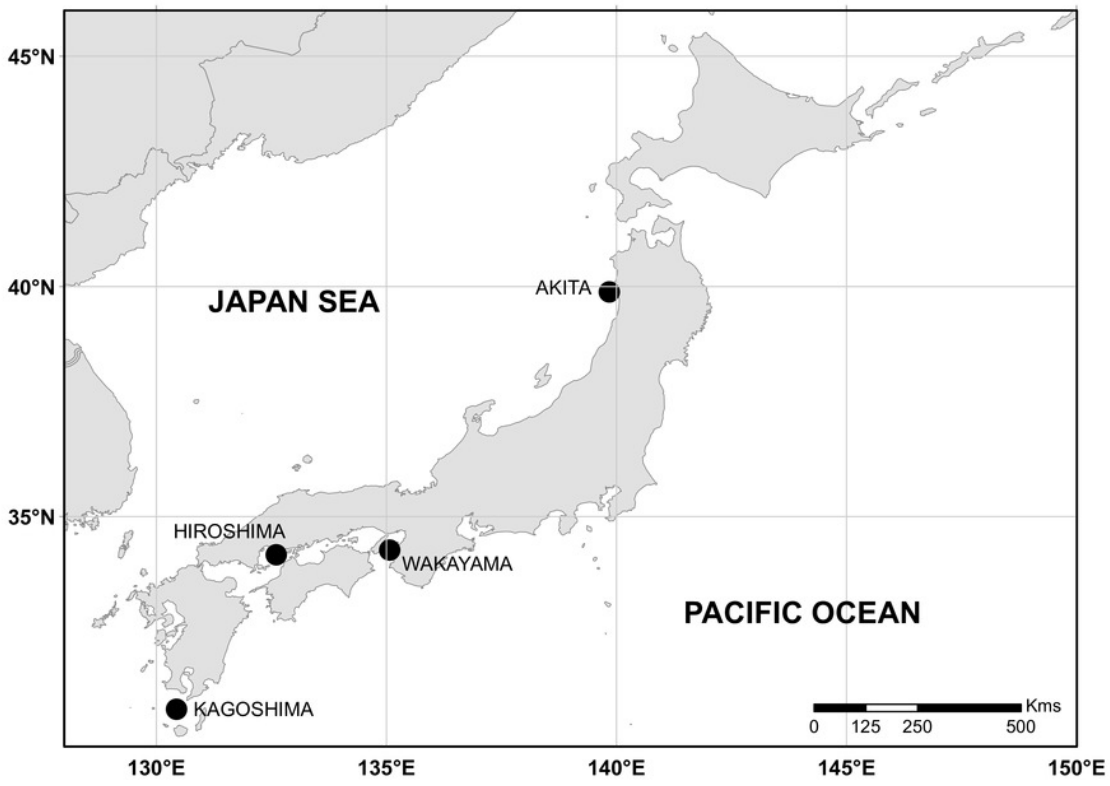

Figure 2

Colouration patterns, meristic counts, and otolith weight ~ age relationships of the three rockfishes *Sebastes cheni*, *Sebastes inermis*, and *Sebastes ventricosus*, and the putative morphological hybrids between them.

The frequency distributions of the number of pored lateral line scales (SLL), number of gill rakers of the first arch (GR), and number of radials of the pectoral fin (PFR) are indicated in each species and putative morphological hybrid. Reference sizes for frequencies are indicated below the three variables. Points in the otolith weight ~ age plot were coloured to ease distinction of species and putative morphological hybrids. Arrows connecting specimens indicate the hypothetical origin of each putative morphological hybrids. A scale of 3 cm was added next to each specimen as reference for size.

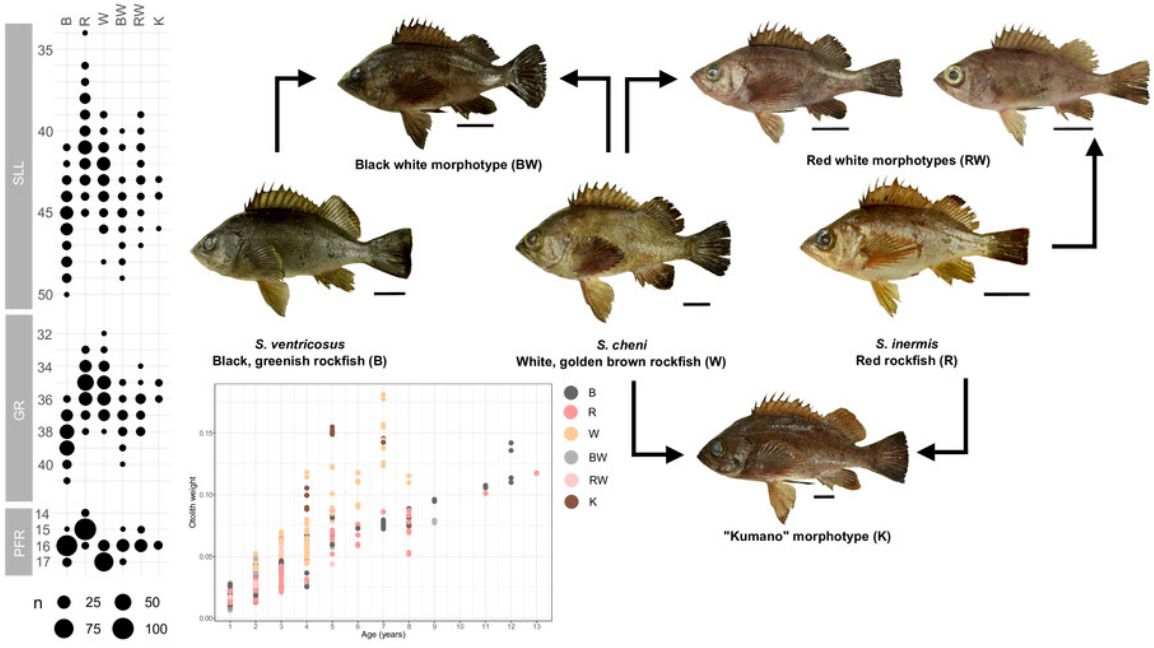
B
R
W
BW
RW
K
SLL
GR
PFR
35
40
45
50
32
34
36
38
40
14
15
16
17
n
25
50
75
100
Black white morphotype (BW)
Red white morphotypes (RW)
S. ventricosus
Black, greenish rockfish (B)
S. cheni
White, golden brown rockfish (W)
S. inermis
Red rockfish (R)
"Kumano" morphotype (K)
Otolith weight
Age (years)

Figure 3

Genetic clusters inferred in the *Sebastes inermis* complex using ten (above and middle) and eight microsatellite loci (above).

Individuals are coloured based on the percentage of their ancestry coefficients (Q-score) for each genetic cluster. Putative morphological hybrids are indicated as K ("Kumano"), BW (*S. cheni* – *S. ventricosus* morphotype), and RW (*S. cheni* – *S. inermis* morphotype).

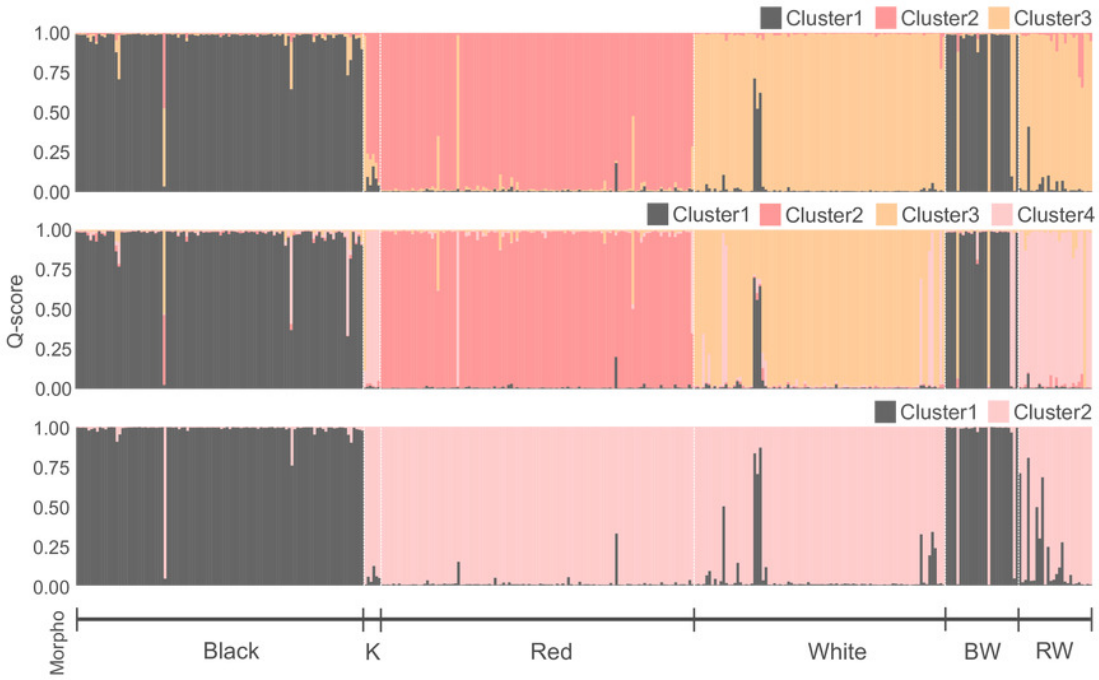

Figure 4

Distribution of maximum Q-scores calculated by STRUCTURE from the observed and simulated individuals separated by the bold vertical dashed line.

Central bold lines in the box plot indicate the medians; box limits represent the 1st and 3rd quartiles; Q-scores are drawn as black circles. Different colours indicate whether boxplots are from pure, hybrids, or backcrosses as represented in the legend above. B: black rockfishes (*S. ventricosus*), R: red rockfishes (*S. inermis*), W: white rockfishes (*S. cheni*), K: “Kumano” morphotype, BW: black-white hybrids, BR: black-red hybrids, and RW: red-white hybrids. Backcrosses are represented with three letters, the first two indicate the F1 hybrid parental and the third one the pure parental. Thus, for example BRB: backcrosses from black-red F1 hybrids and pure black individuals.

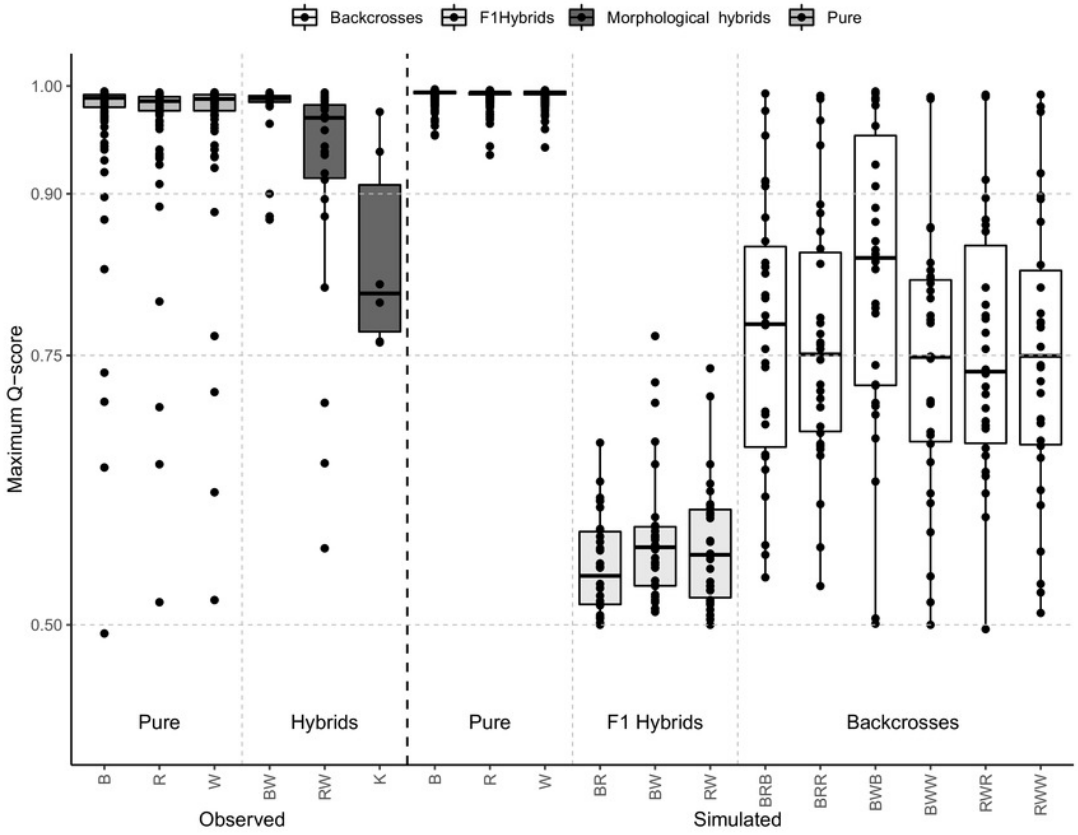
Backcrosses
F1Hybrids
Morphological hybrids
Pure
Maximum Q−score
1.00
0.90
0.75
0.50
Pure
Hybrids
Pure
F1 Hybrids
Backcrosses
B
R
W
BW
RW
K
B
R
W
BR
BW
RW
BRB
BRR
BWB
BWW
RWR
RWW
Observed
Simulated

Figure 5

Haplotype networks constructed from partial sequences of the mitochondrial control region (A) and the intron-free rhodopsin gene (B).

Colours indicate individuals assigned to a single species considering morphological and genetic information. BB, RR, and WW designate individuals identified as *S. ventricosus* (black rockfish), *S. inermis* (red rockfish) and *S. cheni* (white rockfish), respectively, in morphological and genetic analyses. BH, RH, and WH indicate individuals morphologically identified as black, red, and white rockfishes, respectively, but genetically classified as putative hybrids. BW and RW indicate specimens classified as putative morphological hybrids of black-white and red-white rockfishes based on their intermediate morphotypes. K designate to individuals from the “Kumano” morphotype collected off Wakayama.

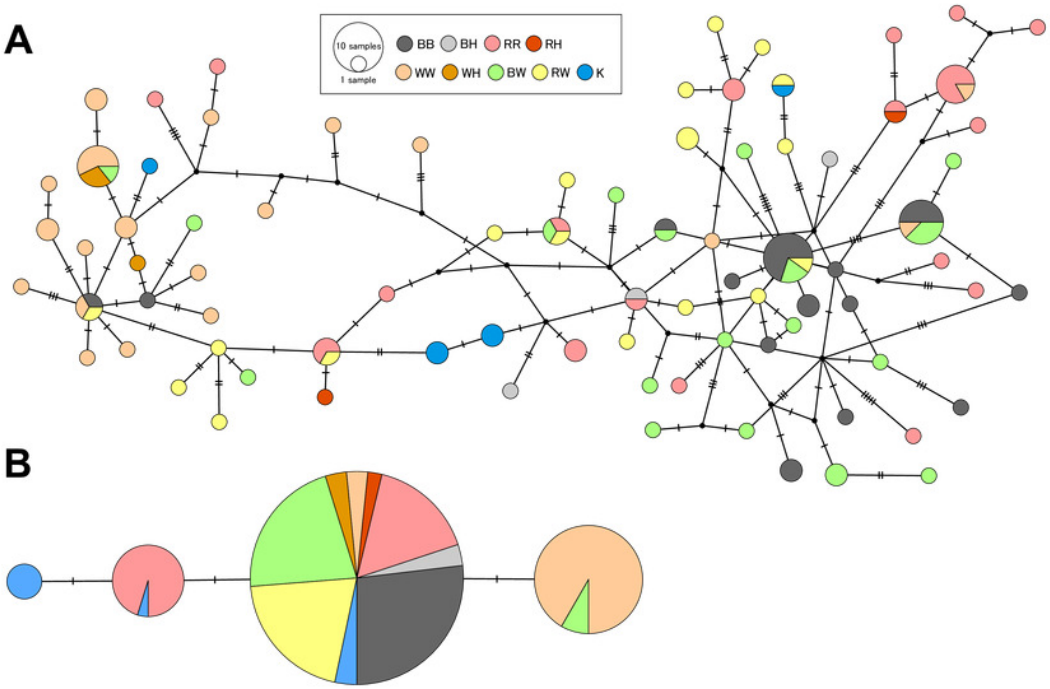
A
10 samples
1 sample
BB
BH
RR
RH
WW
WH
BW
RW
K
B

Table 1(on next page)

Number of samples of each species and putative morphological hybrid collected in each sampling location.

Black-white and red-white putative morphological hybrids are indicated as *S. cheni – S. ventricosus* and *S. cheni – S. Inermis*, respectively.

1

Morphotype	Akita	Hiroshima	Kagoshima	Wakayama	Total
S. ventricosus		41	28	33	102
S. inermis		42	32	37	111
S. cheni	30	43	3	13	89
S. cheni – S. ventricosus		22	1	3	26
S. cheni – S. inermis		19	7		26
Kumano				6	6
Total	30	167	71	94	360

2

3

4

5

6

7

8

Table 2(on next page)

Descriptive statistics for each microsatellite locus in the three species.

N: sample size, Na: number of alleles, Ho: observed heterozygosity, and He: expected heterozygosity. Loci in bold font are under putative divergent selection.

1

	S. cheni (N = 86)			*S. inermis* (N = 111)			*S. ventricosus* (N = 102)		
Locus	Na	Ho	He	Na	Ho	He	Na	Ho	He
SSC12	7	0.539	0.531	8	0.703	0.743	6	0.725	0.726
Seb1	8	0.730	0.672	26	0.631	0.654	70	0.951	0.971
KSs2	17	0.719	0.746	41	0.730	0.931	22	0.775	0.903
Sebi3	18	0.888	0.893	11	0.838	0.855	15	0.912	0.889
SSC23	8	0.629	0.605	14	0.838	0.798	9	0.696	0.727
KSs7	6	0.494	0.581	10	0.622	0.722	7	0.657	0.485
Sebi2	6	0.348	0.366	6	0.559	0.551	5	0.500	0.558
SRA7-7	16	0.876	0.873	15	0.793	0.830	15	0.804	0.838
KSs6	21	0.831	0.895	14	0.892	0.898	15	0.765	0.848
CGN1	11	0.584	0.752	8	0.649	0.679	6	0.480	0.594
Mean	11.8	0.664	0.691	15.3	0.725	0.766	17	0.726	0.754

2

3

4

5

6

Table 3(on next page)

Genetic distances (FST) estimated from D-loop sequences (below diagonal) and 10 microsatellite loci (above diagonal) using genetically pure individuals of each species and putative morphological hybrids collected off Hiroshima

Bold values indicate statistical significance (P value < 0.005).

1

	S. ventricosus	*S. inermis*	*S. cheni*	Black-white	Red-white
S. ventricosus		**0.149**	**0.158**	0.011	**0.136**
S. inermis	**0.119**		**0.118**	**0.127**	**0.138**
S. cheni	**0.358**	**0.235**		**0.111**	**0.091**
Black-white	0.003	**0.104**	**0.254**		**0.087**
Red-white	**0.204**	**0.113**	**0.187**	**0.124**	

2

3

4